

**This paper is being withdrawn from
arXiv due to further data analysis.
Thank you for your interest and stay
tuned!**

A comparison of sports-related head accelerations with and without direct head impacts

Samuel J. Raymond^{1#}, Yuzhe Liu¹, Nicholas J. Cecchi¹, Eli Rice², Ashlyn A. Callan¹, Landon P. Watson¹, Sohrab Sami², Zhou Zhou^{1,3}, Xiaogai Li³, Svein Kleiven³, Michael Zeineh⁴, David B. Camarillo¹

¹ Department of Bioengineering, Stanford University, Stanford, CA, 94305, USA.

² Stanford Center for Clinical Research, Stanford University, Stanford, CA, 94305, USA.

³ Neuronic Engineering, KTH Royal Institute of Technology, Stockholm, 14152, Sweden.

⁴ Department of Radiology, Stanford University, Stanford, CA, 94305, USA.

Corresponding author (e-mail: sjray@stanford.edu)

Abstract

Concussion and repeated exposure to mild traumatic brain injury are risks for athletes in many sports. While direct head impacts are analyzed to improve the detection and awareness of head acceleration events so that an athlete's brain health can be appropriately monitored and treated. However, head accelerations can also be induced by impacts with little or no head involvement. In this work we evaluated if impacts that do not involve direct head contact, such as being pushed in the torso, can be sufficient in collegiate American football to induce head accelerations comparable to direct head impacts. Datasets of impacts with and without direct head contact were collected and compared. These datasets were gathered using a state-of-the-art impact detection algorithm embedded in an instrumented mouthguard to record head kinematics. Video analysis was used to differentiate between impact types. In total, 15 impacts of each type were used in comparison, with clear video screenshots available to distinguish each impact type. Analysis of the kinematics showed that the impacts without direct head contact achieved similar levels of linear and angular accelerations during impact compared to those from direct head impacts. Finite element analyses using the median and peak kinematic signals were used to calculate maximum principal strain of the brain. Statistical analysis revealed that no significant difference was found between the two datasets based on a Bonferroni-adjusted p-value threshold of 0.017, with the exception of peak linear acceleration. Impacts without direct head contact showed higher mean values of peak linear acceleration values of 17.6 g compared to the direct-head impact mean value of 6.1g. These results indicated that impacts other than direct head impacts could still

produce meaningful kinematic loads in the head and as such should be included in athlete health monitoring.

Keywords

Instrumented mouthguard, traumatic brain injury, American football, concussion, brain injury criterion

1. Introduction

Concussion and traumatic brain injuries (TBIs) represent serious health consequences for athletes in sports such as American football ¹. During contact play, players' heads experience accelerations that result in internal strains within the brain ², which can result in physiological damage. While direct head impacts are the primary source of such injuries, further research has pointed to additional sources of these injuries ³. Impacts that do not involve direct head contact may be a potential source of mild TBI (mTBI) ⁴. mTBI may lead to neurodegenerative diseases after repeated exposure to impacts ⁵. Due to its mild nature, it is difficult to detect mTBI and subsequently determine whether or not a player was involved in a sufficiently serious collision. This makes mTBI-causing impacts difficult to observe during a game or practice session based on real-time or video analysis alone ⁶. If impacts that do not involve direct head contact are also a potential source of mTBI, this problem is compounded as these impacts are most likely ignored by those monitoring athlete health. Attaching sensors to players to record their kinematics is one approach that can increase the ability to detect mTBI in sports ⁷. Instrumented mouthguards, in particular, have been used in the past to great effect in gathering data on athlete head kinematics and to develop models of the effect on the physiology of the player ⁸. Mouthguards are well suited to track head motion as they are fitted to the upper dentition, and therefore rigidly connected to the skull. With this additional source of data, combined with video analysis and player interviews, the study of head impacts, concussion, and mTBI has resulted in a number of key insights to help improve helmet design and safety ⁹. However, consensus as to the threat of impacts without direct head contact has not been reached, and the current approach is to ignore these impacts in sports. In their work Lessley et al. ¹⁰ analyzed impacts to the helmet that resulted in concussion, finding body impacts to the helmet were the most common cause. This is likely due to the momentum transfer difference between hitting helmet to helmet or helmet to body, the latter representing a more unbalanced impact in favor of the body. However, their analysis did not report findings on impacts where the head was not involved at all and only players' bodies were involved. In another work by Lessley et al. ¹¹ the position-specific nature of concussions in the NFL was analyzed and found that helmet to ground impacts were among the most frequent causes of concussions. While these works focused on the diagnosed injuries resulting from direct head impact, little has been discovered as to the effect of repeated, lower intensity impacts that can result when there is no direct head contact.

For a brain to undergo the dynamics that can result in mTBI, sufficient momentum is required to be transferred from the skull to the brain to induce motion ¹². For injuries to occur, this motion threshold is associated with the angular and linear accelerations to which the skull is subjected. While in practice, there are correlations between impact location and mTBI sensitivity, in theory the source and location of the accelerations is not relevant to whether or not mTBI can be generated. So long as sufficient impulse travels to the skull, the brain may be accelerated such that mTBI can occur. In the analysis conducted by Smith et al. ¹³ a combination of direct and indirect loading to headforms was numerically studied using finite element analysis (FEA). They found that indirect impacts could produce significant values of angular acceleration, a variable that is closely correlated with brain injury. For direct head impacts, the close proximity of the source may make it easier to reach the threshold for mTBI, however for an impact to other parts of the body, there are still many common situations in human movement where the necessary mTBI head accelerations can be achieved. In the field of sports-related concussion, McCrory et al. ¹⁴ provided a consensus statement that acknowledges that impacts near the head (neck, face, shoulder) and elsewhere on the body can result in significant impulses transmitted to the brain. Indirect impacts have also been studied in men's soccer ¹⁵ by Cassoudealle et al., where head-to-head was used as the primary indicator to classify an impact. In their work they report 3% of the concussions analyzed were caused by indirect impacts. In a non-contact sport like soccer, the present focus on impacts without direct head contact is of potentially considerable importance. In women's high school lacrosse, Caswell et al. ¹⁶ reported that, after video verification, nearly 75% of the impacts detected by head acceleration sensors were produced without direct head impact events, highlighting the vast contrast in the number of impacts that can occur without direct head involvement. Similar results for women's collegiate lacrosse were found in Cecchi et al. ¹⁷. In Jadischke et al. ¹⁸ laboratory experiments were performed to analyze chest impacts on players' cervical spinal cord, finding lower head accelerations when compared to direct helmet-to-helmet collisions. However, the authors suggest that spinal cord tension during body impacts could be a contributing factor to concussion that would evade current sensor measurements. The growing body of work, therefore, is starting to reveal that, while direct head impacts typically yield the highest head accelerations, other types of impacts may be far more common, and potentially significant enough to warrant the same level of monitoring during game play.

In this work we present findings that indicate that impacts without direct head contact can result in sufficient loading to the brain to induce high-velocity impacts that do not cause concussion, but that may increase the likelihood of mTBI. Using a combination of video analysis, a deep learning-based impact detection algorithm, and a detailed finite element model using the kinematic data from an instrumented mouthguard, we compared the results of impacts with and without direct head contact on the brain. We describe the methods involved in gathering the data and classifying the impacts, as well as the numerical techniques used to calculate the strains in the brain matter for each impact type. Following this the results of our study are presented, and finally a discussion of the importance of monitoring all impacts in sports concludes the paper.

2. Methods

In this section we describe the procedures implemented to gather the two datasets used to represent impacts with and without direct head contact. Our instrumented mouthguard and impact detection system is briefly introduced, followed by our video verification workflow to determine which type each impact was, and finally the FEA model used to calculate brain strain values from the recorded head kinematics.

2.1 Instrumented Mouthguard and Impact Detection

Stanford Mouthguard

To capture the kinematics of the players during game play, the instrumented Stanford Mouthguard MiG2.0¹⁹ was used to measure linear and angular head kinematics during an impact. The device is capable of sensing six degrees of freedom kinematics via a triaxial accelerometer with maximum range of +/-400 g, and a triaxial gyroscope with maximum range of +/-4000 degrees/sec. Linear acceleration was acquired at 1000 Hz, while angular velocity was acquired at 8000Hz. When the linear acceleration threshold value set by the user is crossed at any of the linear acceleration components, an event is written to the on-board flash memory chip. The triggering threshold in this study was 10 g, and all recorded events contained 50 ms of data pre-trigger and 150 ms post-trigger. Trigger threshold, pre- and post-trigger recording time windows, event duration, and sample rate of the inertial measurement units (IMUs) were user adjustable. The kinematic data was stored in comma separated value (CSV) format using the recommended common data elements (CDE) from the National Institute of Neurological Disorders and Strokes (NINDS) for collecting sensor data²⁰. After games and practices, these mouthguards were collected, and the data transferred to the MiG2.0 website for processing and analysis with our MiGNet Impact Detector algorithm.

MiGNet Impact Detector

The MiGNet Impact Detector algorithm is a deep learning model trained to differentiate between true and false impact kinematic data. The kinematic data collected was in the form of 6 1x200ms time series signals, each representing a kinematic variable (3-linear and 3-angular accelerations) in one spatial dimension. The model was a deep convolutional neural network trained on a large dataset of video verified signals, more details can be found in²⁰. Further improvements to this model were introduced such that this model offers positive predictive values and negative predictive values of 88% and 83%, respectively. This MiGNet 2.0, improved with physics-informed machine learning^{21,22} is a potential replacement for traditional video analysis. However, as we required the type of impact to also be determined, further video analysis of the detected impacts was also conducted.

2.2 Video Analysis

Video Capture

Practice and game footage of participants was collected by experienced videographers using four cameras at 1080p and 60 fps. Video was taken at four angles simultaneously from a high position: (a) Near Sideline, (b) Far Sideline, (c) Left Endzone, and (d) Right Endzone. To enable synchronization with the recorded data from the mouthguards, each camera angle had footage of a world clock visible at the beginning of the practice. Videos were intended to capture separated periods of active game play, including plays and drills, with passive time periods not filmed. During these active periods, the camera's field of view panned to follow the ball, at times excluding mouthguard instrumented participants from the frame.

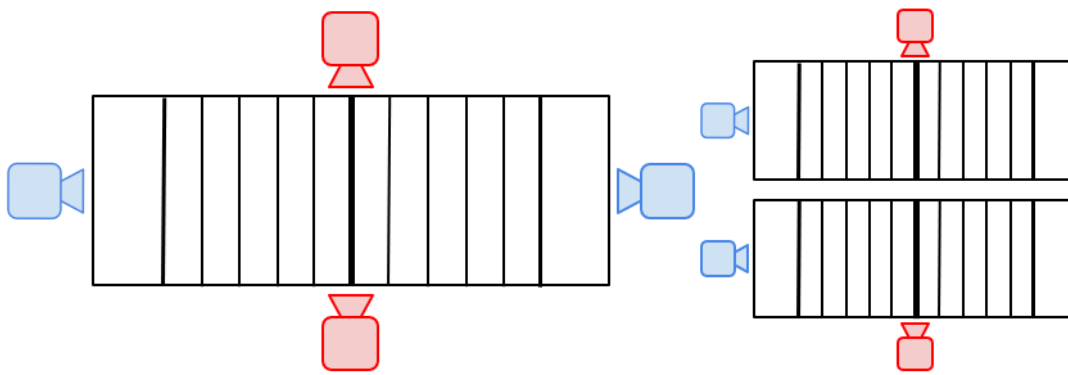


Figure 1 – (Left) Potential camera location positions for video analysis of game play. Two cameras shown for both sideline and end zone on the diagram to show both of the possibilities, as the side that the camera was on would depend on the practice. (Right) An example of what the camera angles could look like.

Figure 1 depicts the locations of the cameras that recorded the footage used. When two fields were utilized in their practice, each field had one camera on one of the sidelines (red) and one on one of the endzones (blue). The camera angles were also not necessarily consistent between the two fields.

Video Verification

Two video reviewers were trained to review impact events on video²³. The reviewers were given access to the mouthguard-collected kinematic data, corresponding video, and participant identification data. Each reviewer focused on one participant during one specific game or practice at a time. The mouthguard kinematic data provided the timestamp for each impact event for a specific participant. All camera angles were viewed to track the activity of their assigned participant for that given practice or game with the purpose of matching the timestamp of the video with that of the corresponding kinematic data. At these synchronized points in time, the reviewers observed the activity of the

participant and classified it with three distinct labels: direct head impact, impacts without direct head contact, and non-impact. Non-impacts were not analyzed as they represent false positives in the impact detection. For data clarification non-impacts were labeled accordingly: No Contact, Obstructed View, Not in Frame, User Error, and Device Error.

An impact event was defined as a physical interaction with either an opposing player, a teammate, or the playing surface. A direct head impact classification was defined as an observed activity in which the mouthguard-instrumented participant sustained direct contact with another athlete's helmet above the shoulders. When an impact was observed in which the mouthguard-instrumented participant received an impact event at the shoulders or below, this was classified as an impact without direct head contact.

For the Non-impact cases: a *No Contact* classification was defined as situations when the participant was observed within the video frame but did not experience external contact at the given timestamp. An *Obstructed View* classification was defined when the participant was observed within the video frame, but the nature of their activity was obstructed and/or ambiguous at the given timestamp. A *Not in Frame* classification was defined when the participant was not visible in the video frame at the given timestamp. A *User Error* classification was defined as situations in which improper use of the mouthguard by participants was present, such as when participants chewed on the mouthguard or placed it in their pocket or sock. User Error classifications were confirmed through corroborating video evidence, participant testimonial, and signature data output patterns. Certain kinematics patterns have shown correlation with placement of mouthguard in a participant's sock and consist of multiple impacts within a short time frame. Participants outputting such data patterns, if lacking testimonial confirmation of improper mouthguard use, were typically confirmed via video evidence to be running or walking without external contact during the relevant timeframe. Finally, a *Device Error* classification was defined as situations in which the hardware or software of the MiG 2.0 Mouthguard workflow failed in a given capacity. Furthermore, an *Unclear Timing* classification was defined as situations where the participant is observed on video to have experienced multiple incidents of external contact during a short time frame. In these situations, the video reviewer may not be able to determine with certainty which observed impact event correlates to a given kinematic data output. This labeling also includes the inverse scenario, when there are instead multiple kinematic data outputs during a short time frame, and it is uncertain which kinematic data output correlates to a given video observed impact event. All Non-impact classifications were excluded from analysis. However, the effort used to classify these Non-impact events was important for additional scrutiny and to aid the improvement of the MiGNet 2.0 impact detector.

After the classification of the participants' activity at each timestamp, a series of still images depicting the impact were captured, an example of the two impact types is shown in Figure 2.

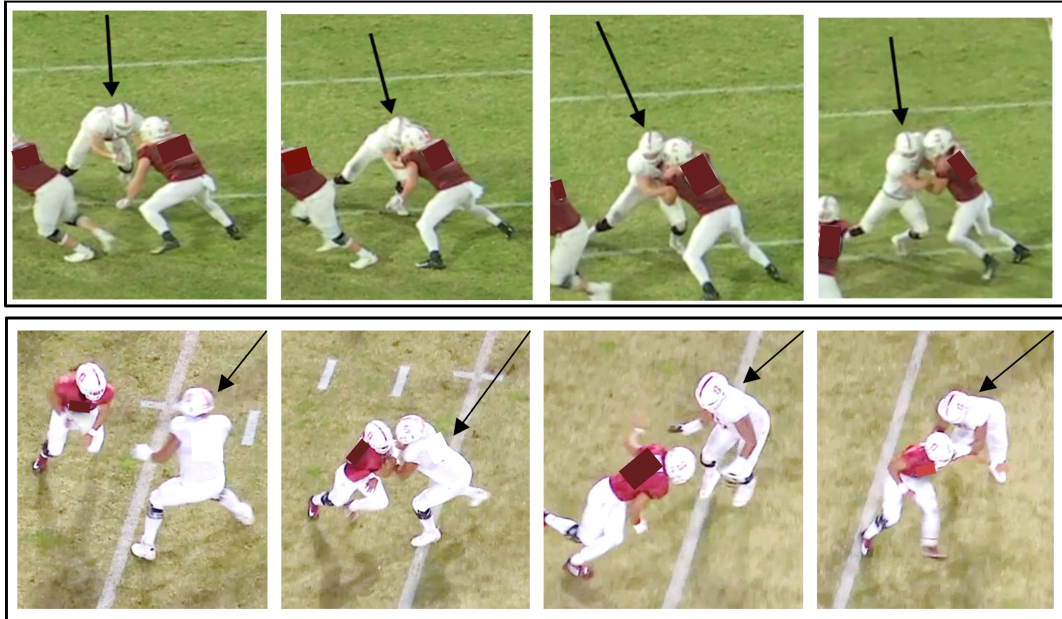


Figure 2 - A series of screenshots showing the impact event captured on video and used for classification. (Top) An event that was classified as a direct head impact. (Bottom) An event that was classified as an impact without direct head contact.

Verified Impact Dataset

In total, 5,617 impact events were recorded in 22 practice sessions over a three-month period in the Fall of 2019. After an initial video review, where impact type was not determined, 4780 impact events were found to occur off-screen and as such were removed from the dataset. Of the remaining impacts, 522 were confirmed as non-impacts and 315 were verified impacts. For classification of direct head impacts and impact with no direct head contact, mouthguard files were ranked by event count as this increased the likelihood of the video reviewer finding a passable impact. Any files containing more than 300 events were not analyzed as, anecdotally, this high of an event count for a single session would typically indicate device error. Initially, these files were video analyzed to identify impacts with no direct head contact. After looking through all of the files, 15 body impacts were found that were clear enough to be agreed upon to be collisions with no direct head contact. This process was then repeated until 15 head impacts of similar clarity were found.

2.3 Finite Element Brain Model

KTH Finite Element Brain Model

In this study, the FE model developed at the Royal Institute of Technology (KTH) ²⁴ was used with LS-DYNA software to calculate the brain strain resulting from each impact. In the KTH model the brain included cerebral gray matter, cerebral white matter, cerebellum, corpus callosum, midbrain, thalamus, and brainstem. In total 4124 elements were used to

represent the brain. As the structure of interest in the current study, the brain is simulated as an isotropic and homogeneous object, in which a second order hyperelastic constitutive law was employed to describe its nonlinear behavior with additional linear viscoelastic terms to account for its rate dependence ²⁴. The KTH FE model was validated by previous experiment results including brain-skull relative motion ²⁵, intracranial pressure ²⁶, and brain strain ²⁷, brain-skull relative motion ²⁵, intracranial pressure ²⁶, and brain strain ²⁷.

In these simulations, the skull was assumed to be rigid and move according to the kinematic data provided by the mouthguard sensors. The brain tissue was deformed by the skull's inertia, and, after completion of the 200ms simulation, the peak maximum principal strain (MPS) was calculated for every element. Then, for each impact, the 95th percentile value of the peak MPS among the whole brain was calculated to indicate the severity of deformation resulting from the impacts. This 95th percentile value of MPS was used in previous works as a proxy to brain injury ^{28,29}. This model was used to analyze all 30 of the impacts collected after video analysis.

Detailed KTH finite element head model

To better compare the two impact types, the median and peak impacts from the two categories were selected and simulated using a more detailed version of the KTH FE model that includes millions instead of thousands of elements. This FE model was recently developed at the Royal Institute of Technology (KTH) in Stockholm ³⁰ using the LS-DYNA software. The detailed KTH FE model includes the brain, skull, meninges (i.e., dura mater, pia mater, falx, and tentorium), subarachnoid CSF, ventricle, and sinuses (i.e., superior sagittal sinus and transverse sinus). The brain was further grouped to have explicit representation of primary subcomponents, including four lobes of the cerebral gray matter (GM) (Figure 3A), cerebellar GM, cerebral white matter (WM), cerebellar WM, and brainstem (Figure 3B). Detailed information regarding the geometry discretization, material choice for each head component as well as the interface conditions among various intracranial components are available in a previous study ³⁰. Responses of the model have shown good correlation with experiments of brain-skull relative motion ²⁵, intracranial pressure ²⁶, and brain strain ²⁷.

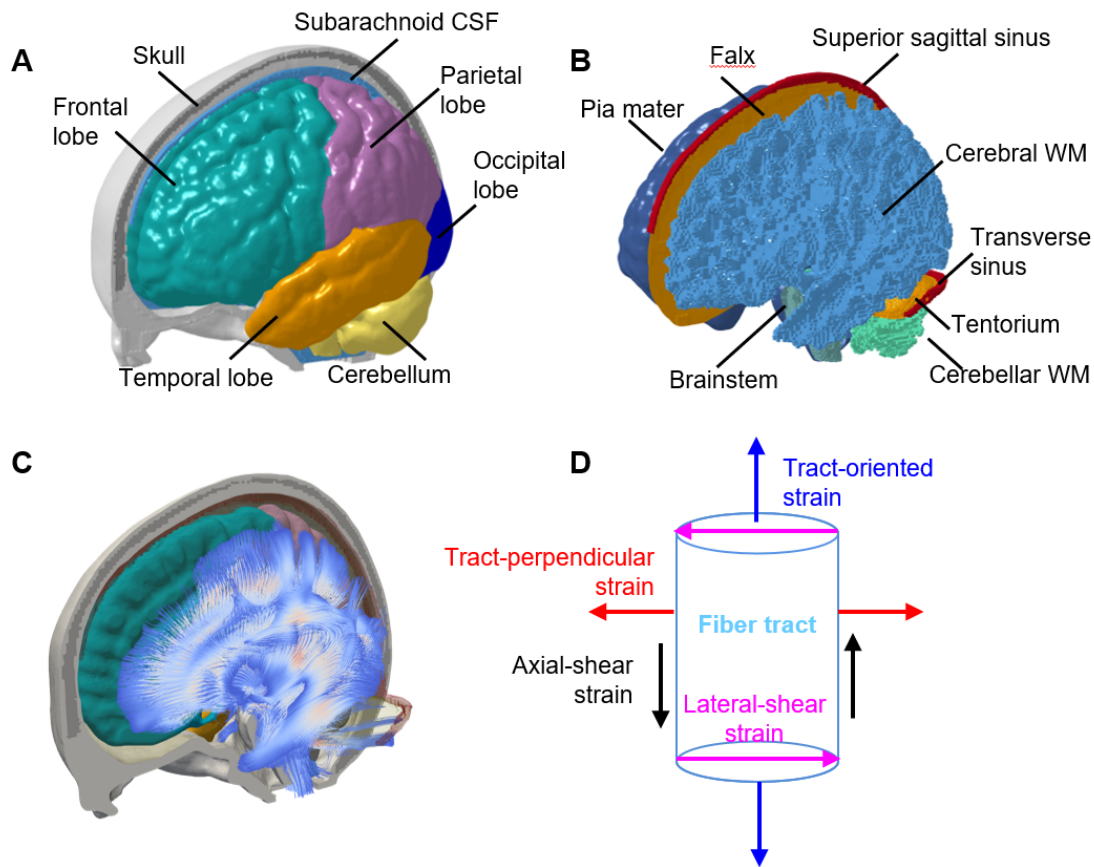


Figure 3 - Finite element model of the human head with embedded truss elements. (A) Finite element model of the human head with the skull open to expose the subarachnoid cerebrospinal fluid (CSF) and brain. **(B)** Model of cerebral white matter (WM), cerebellar WM, brainstem, pia mater, falx, and tentorium. **(C)** View of the brain embedded with axonal fiber tracts. **(D)** Sketch illustrates four tract-related strains with respect to the fiber tract.

To extract the deformation related to the fiber tracts, the primary orientation of WM fiber tracts was extracted from the ICBM DTI-81 atlas and then embedded within the head model following the approaches presented earlier³¹³². For each WM element in the head model, corresponding voxel in the DTI atlas that is closest to the centroid of the given WM element was identified, and the diffusion tensor of the identified voxel was processed to obtain its first principal eigenvector representing the primary fiber orientation for this finite element. The DTI-derived fiber orientation is concretely presented as truss elements, which were embedded within the WM elements (Figure 3C). Note that the embedded truss elements were only used to monitor the dynamically changing local fiber orientation during the head impacts without additional contribution to the mechanical stiffness. Once a simulation is completed, both the Green-Lagrange strain tensor for each WM element and the orientation of its embedded truss element for a given time step were extracted. By transforming the strain tensor to the coordinate systems with one axis aligned with the

real-time fiber orientation, four tract-related strains were obtained, including the tract-oriented strain, tract-perpendicular strain, axial-shear strain, and lateral-shear strain. As illustrated in Figure 3D, these four tract-related strain measures characterize the normal and shear deformation parallel and perpendicular to the fiber tracts, respectively. Technical details regarding the embedded fiber tracts for tracking the dynamic fiber orientation and the computation of four tract-related strains are available in ³¹ and ³², respectively. These more detailed models allowed the comparison of the four cases (2 per category) in more physiological depth.

3. Results

After collecting mouthguard data from the participants, processing with the MiGNet impact detection and classification of the impact type, the datasets were compared and analyzed.

3.1 Impact Dataset

In total, 30 samples of impact events were collected, 15 direct head impacts and 15 without direct head contact. The magnitude of the linear acceleration of these signals are shown in Figure 4 with the direct head impacts on the left and impacts with no head contact on the right. Figure 5 shows the violin plots of the Peak Linear Acceleration (left) and Peak Angular Velocities (right).

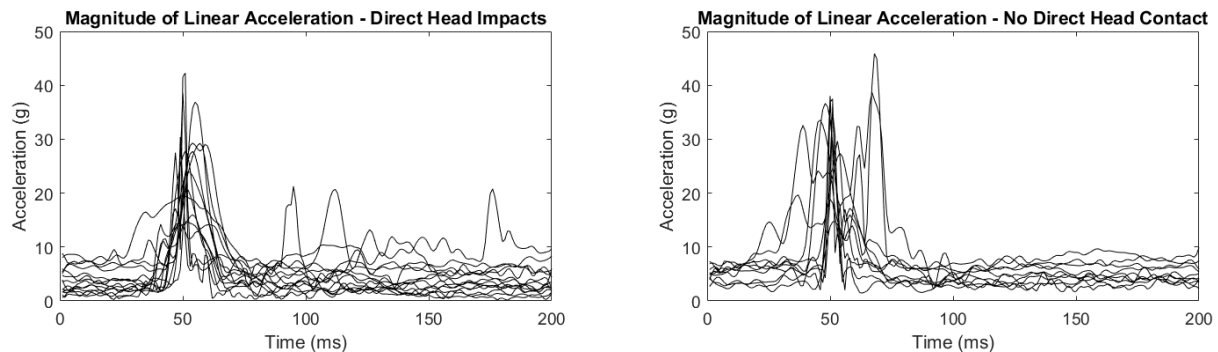


Figure 4 - (Left) Magnitude of linear acceleration for all direct head impacts. (Right) Magnitude of linear acceleration for all impacts with no direct head contact. Note the scale bars are matched.

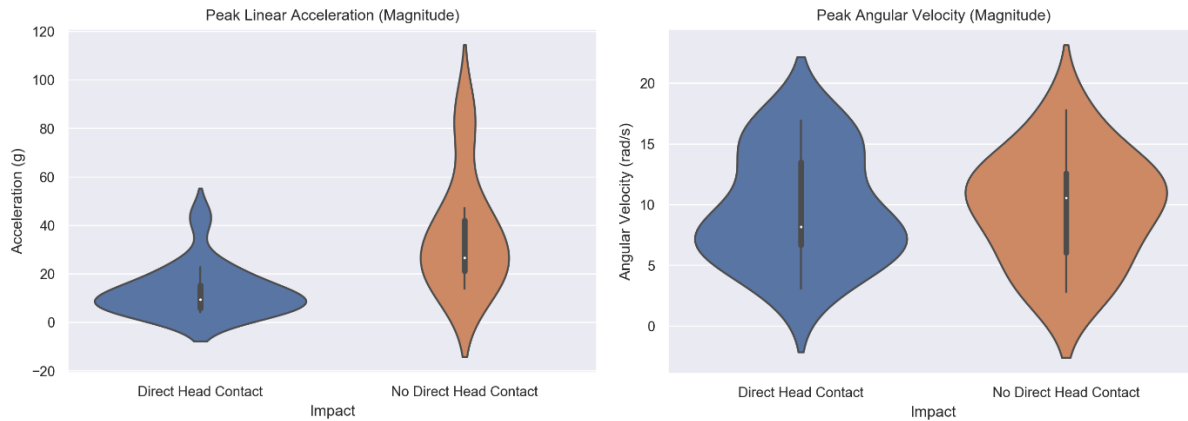


Figure 5 - (Left) Comparison of Peak Linear Acceleration between the two impact types. (Right) Comparison of Peak Angular Velocity between the two impact types.

In addition to the statistical analysis of these datasets, to compare representative signals from each impact category, these signals were then ranked in severity based on the peak linear acceleration values. The signals corresponding to the 50th percentile and 99th percentile severities were then chosen to compare the two datasets.

3.2 Comparison of impact type based on kinematics

The linear and angular acceleration signals are shown in Figure 6 for the 50th percentile direct head impact, Figure 7 for the 99th percentile direct head impact, and Figure 8 and Figure 9 for the impacts with no direct head contact, respectively. For each graph shown the 3 spatial directions are overlaid to see the motion in 3-dimensions as the impact unfolds. Based on a p-value threshold of 0.05, and accounting for the effect of multiple comparisons with Bonferroni corrections, these results show that the mean of the linear acceleration, shown in Figure 5 (left), is higher in the case of no direct head contact with a p-value of <0.001. With a corrected significance value of $0.05/3 \sim 0.017$, this indicates that mean peak linear acceleration is higher in impacts in this dataset with no direct head contact. For the case of angular acceleration, the p-value is 0.231 and thus is not significantly different.

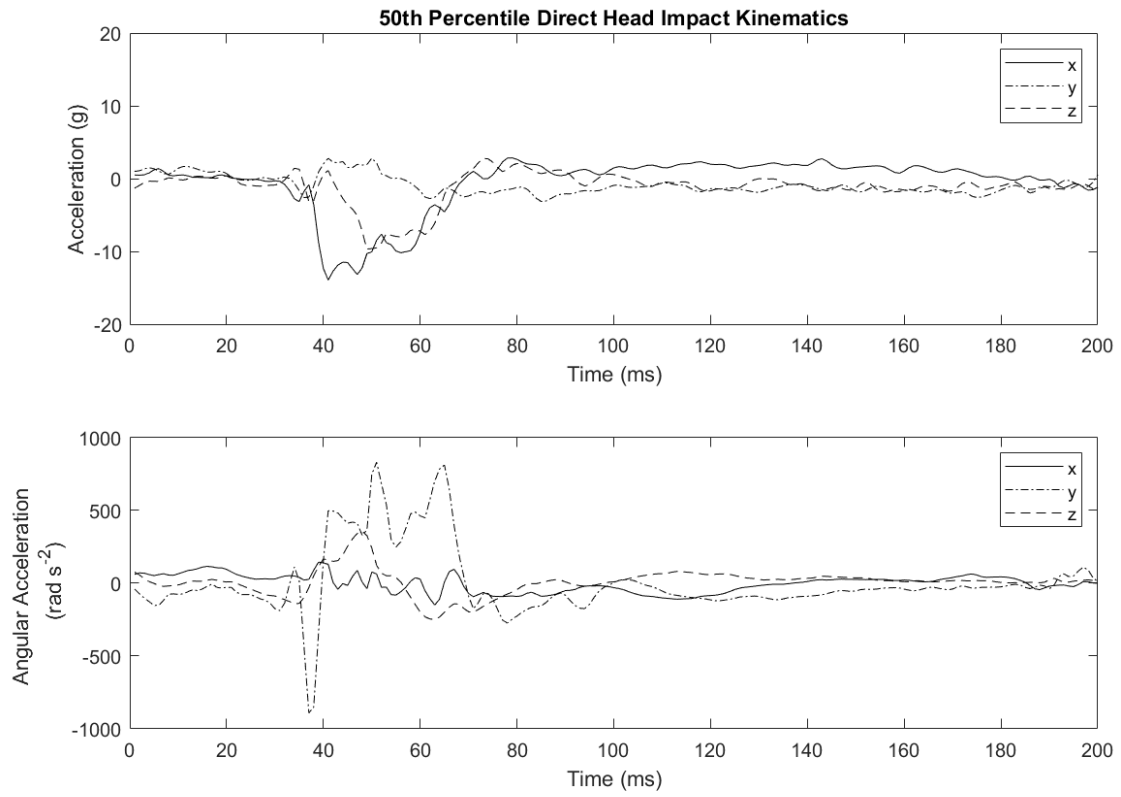


Figure 6 - Direct head impacts.(Top) Linear acceleration for the 50th percentile sample. (Bottom) Angular acceleration for the 50th percentile sample.

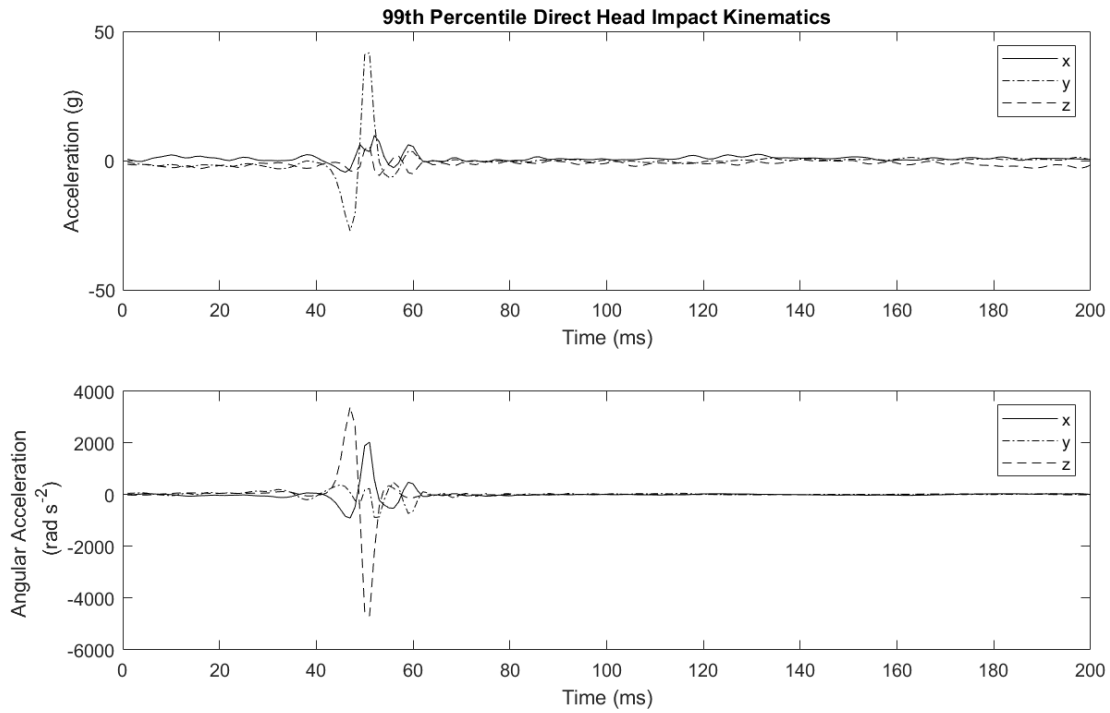


Figure 7 - Direct head impacts. (Top) Linear acceleration for the 99th percentile sample. (Bottom) Angular acceleration for the 99th percentile sample.

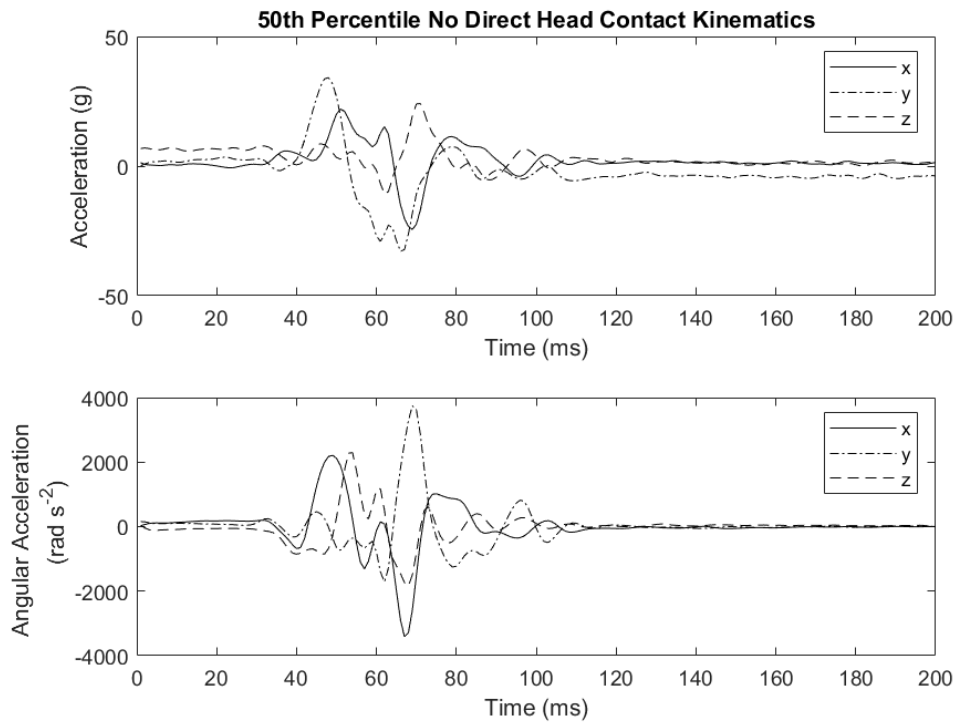


Figure 8 - Impacts with no direct head contact. (Top) Linear acceleration for the 50th percentile sample. (Bottom) Angular acceleration for the 50th percentile sample.

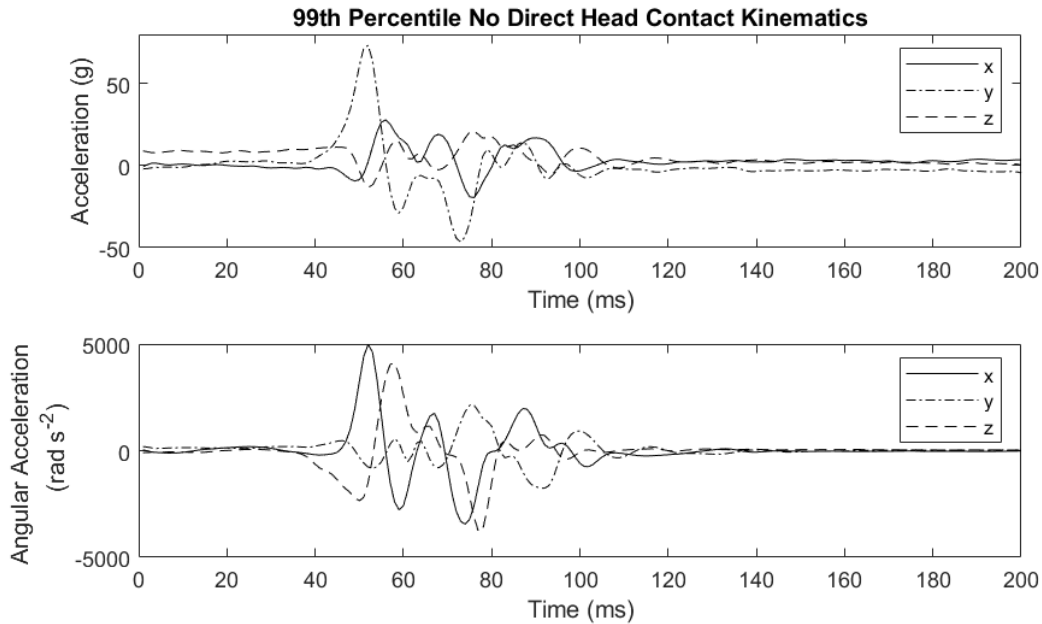


Figure 9 - Impacts with no direct head contact. (Top) Linear acceleration for the 99th percentile sample. (Bottom) Angular acceleration for the 99th percentile sample.

3.3 FEM Results

While kinematic data is valuable as an initial screening for impact severity, utilizing these kinematics signals as input to an FEM brain model allowed for the calculation of induced brain strain values. These values are often used to compare injury metrics and to inform physiological damage^{19,28,29}.

KTH finite element head model

Using the KTH FE model described in the initial part of Section 2.3, the peak maximum principal strain values (MPS) were extracted from all 30 impact models. These are shown for direct head impacts in Figure 10 (left) and impacts with no head contact (right). Violin plots for the 95th percentile MPS values are shown in Figure 11.

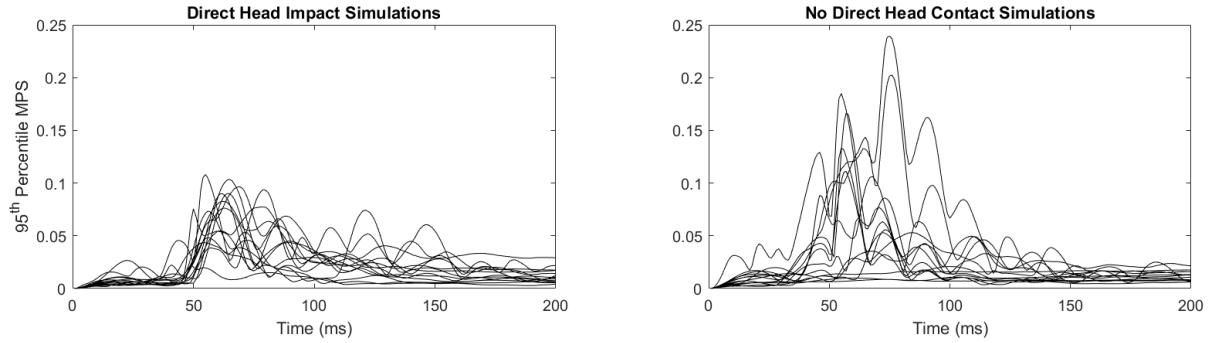


Figure 10 - (Left) Peak maximum principal strains as a function of time over all for the direct head impact simulations. (Right) The same for the models with no direct head contact.

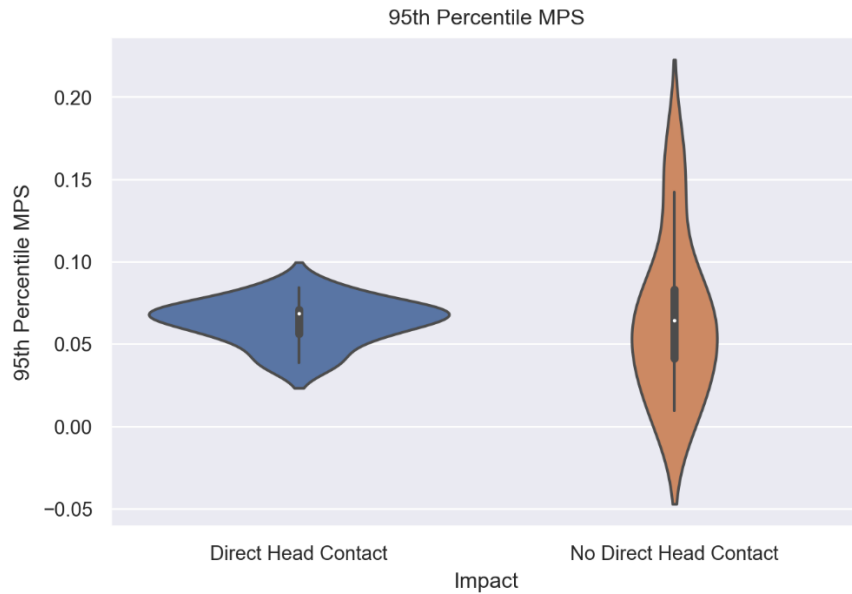


Figure 11 - Comparison of distributions for MPS values for both impact types.

The representative 50th and 99th percentile simulation results for the direct head impact simulations showing the MPS evolutions are shown in Figure 12. For impacts with no head contact, these are shown in Figure 13. In addition, for this KTH model, the spatial distribution of the MPS for the two direct impact models and the two models with no head contact are shown in Figure 14 and Figure 15.

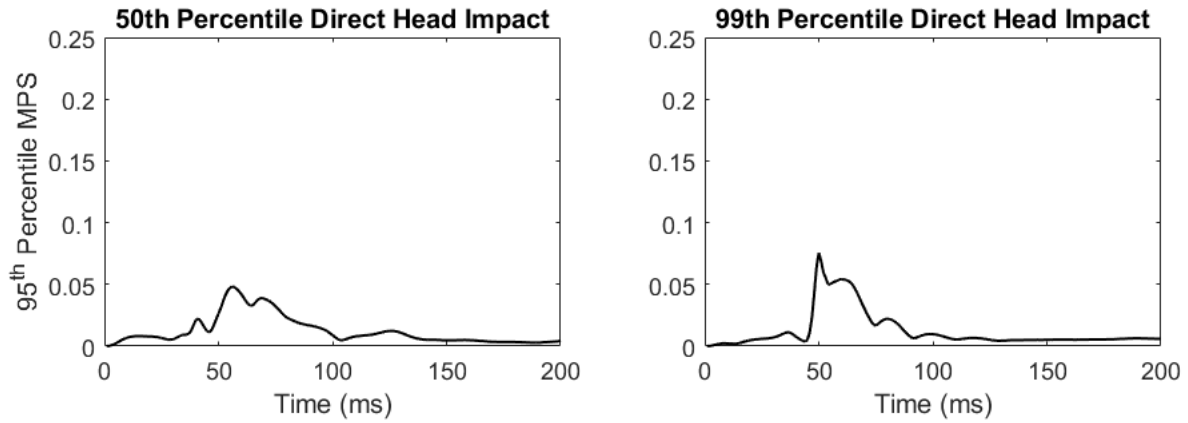


Figure 12 - Direct head impact. (Left) 50th percentile MPS results from the KTH model. (Right) 99th percentile MPS results from the KTH model.

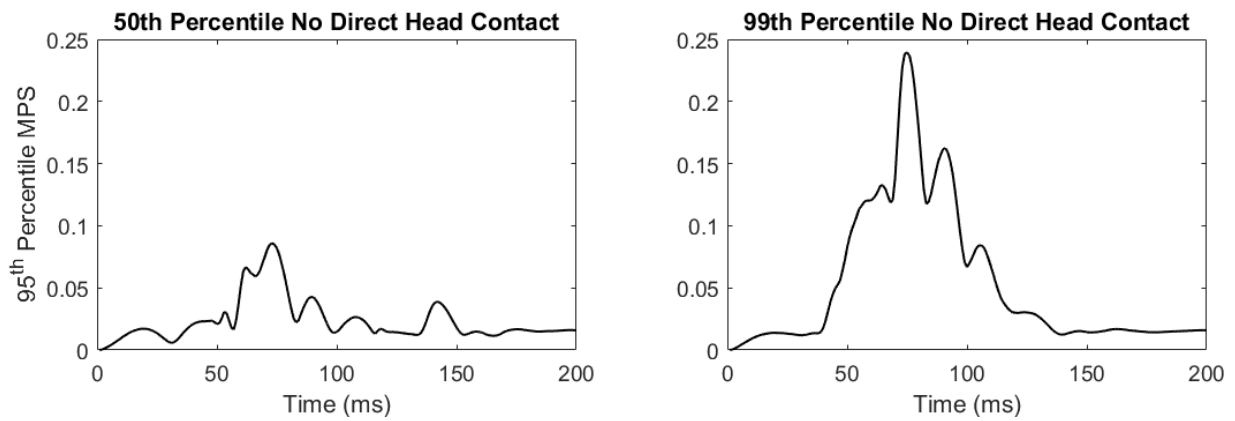


Figure 13 - Impacts with no direct head contact.(Left) 50th percentile MPS results from the KTH model. (Right) 99th percentile MPS results from the KTH model.

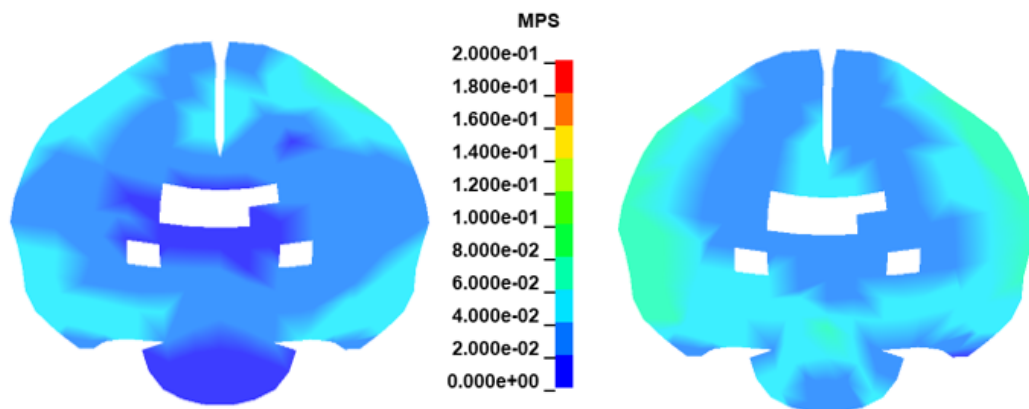


Figure 14 - Impacts with direct head contact(Left) Spatial distribution of the peak MPS values in the 50th percentile. (Right) Spatial distribution of the peak MPS in the 99th percentile.

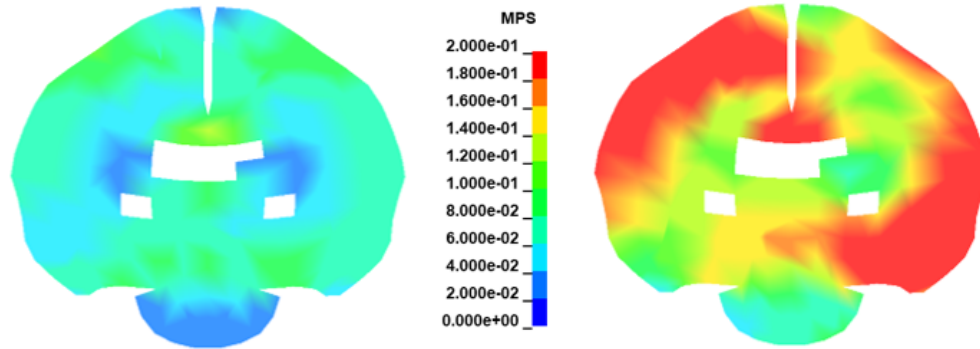


Figure 15 - Impacts with no direct head contact. (Left) Spatial distribution of the peak MPS values in the 50th percentile. (Right) Spatial distribution of the peak MPS in the 99th percentile.

Detailed KTH finite element head model

To further analyze the different impact types on the brain mechanics, the four representative signals were also simulated using the more detailed version of the KTH head FE model, described in the latter part of Section 2.3. These results show the white matter and whole brain MPS values, see Figure 16 and Figure 17.

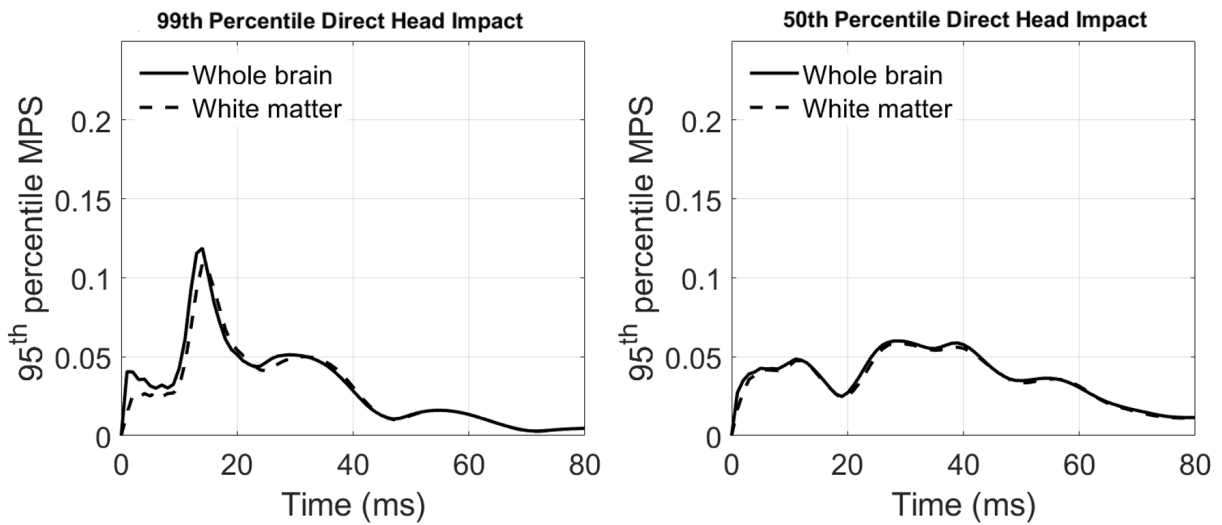


Figure 16 - MPS time history of the direct head impacts using the detailed KTH model showing (left) 99th percentile and (right) 50th percentile impacts.

In addition, these FE models also calculated the directional fiber strains that can develop during head accelerations. The different orientations of these strains are shown in Figure 18 for each of the four examples.

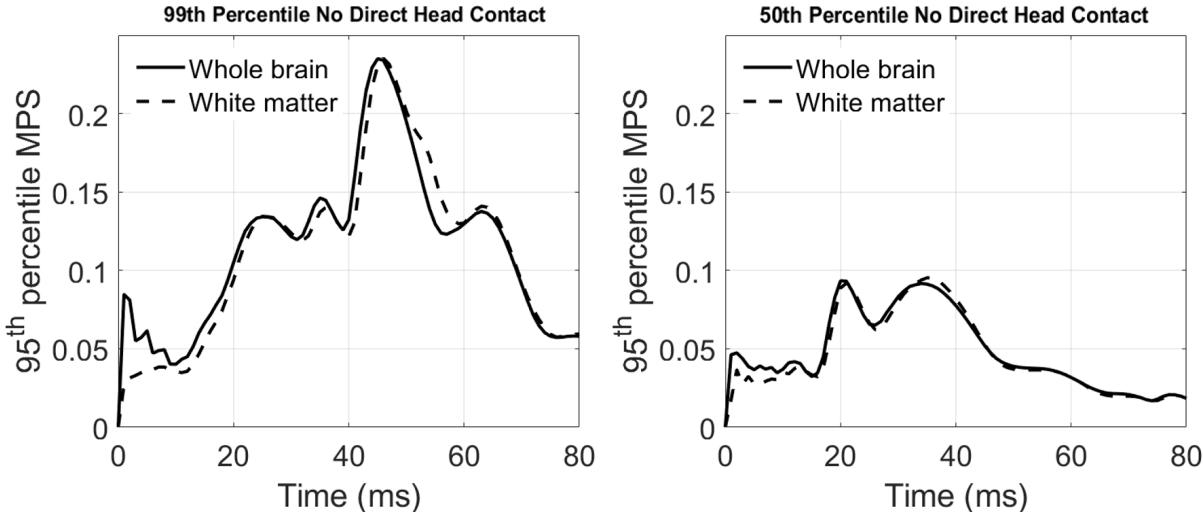


Figure 17 - MPS time history of the impacts with no direct head contact using the detailed KTH model showing (left) 99th percentile and (right) 50th percentile impacts.

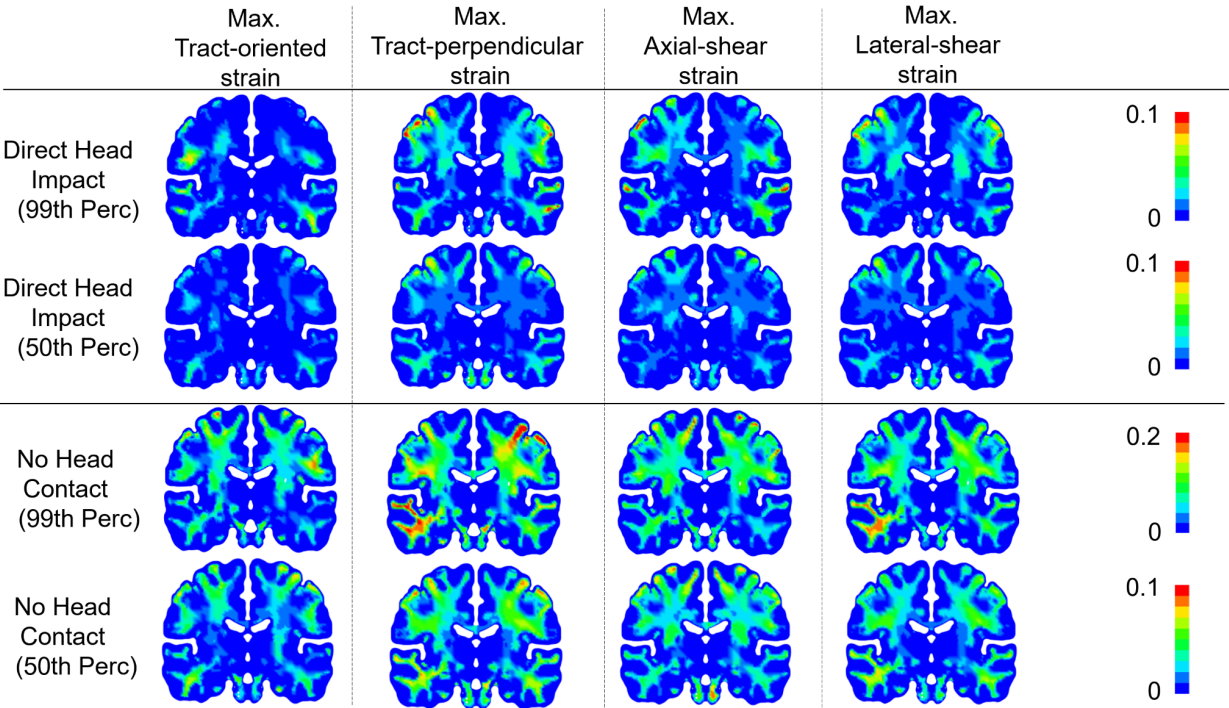


Figure 18 - Fiber-related strain values for the four cases of impacts to the brain.

4. Discussion

In this work we analyzed head kinematic data and video footage of collegiate American football athletes to create two datasets of impacts. These two datasets consisted of impacts from direct head impacts, and impacts from interactions with no direct head contact. Data from players' instrumented mouthguards were analyzed using a state-of-the-art impact detection algorithm based on a physics-informed machine learning model to identify true impact events. For a confirmed impact to be classified as either a direct head impact or an impact with no head contact, further video analysis was required to indicate whether or not the head was involved at all in the impact. Screenshots of the game and practice videos were collected, and a unanimous decision was required amongst 5 video reviewers as to which category each impact belonged. After reviewing over 5000 recorded impacts for clarity and unanimous impact type classification, this resulted in a total of 30 samples, 15 impacts per category. These impact samples consisted of 200ms signals of the linear and angular accelerations and angular velocity in 3-dimensions during the duration of the impact. In addition to the kinematic data, these samples were used to create 30 FEA brain models using the standard KTH head model. Ranking the impacts by the magnitude of peak linear acceleration, the 50th and 99th percentile samples were chosen to represent the two categories. These 4 samples were used as input to a more detailed KTH head model. These simulations were used to predict brain strain values from the impact data.

Figure 5 shows the distribution between the two dataset's kinematics. Using a p-value threshold of 0.05 for significance, an analysis showed no significant differences in peak angular acceleration or 95th percentile MPS. Impacts without direct head contact showed higher mean values of peak linear acceleration values of 17.6 g compared to the direct-head impact mean value of 6.1g with a statistical significance of p-value <0.001. It is important to note that the standard deviation of the impacts with no head contact were consistently 3-times larger than the direct head impact data. This was likely explained by the multitude of collision types that can occur when dealing with impacts other than direct head contact. Given the strict requirements to obtain clear footage of these impacts, it is more than likely that the head impacts found using this filtering represented a milder subset of the general distribution of impact intensities. The important takeaway, however, is that these results showed the two datasets were not significantly different from one another. This implies that impacts of any type, even those with no direct head involvement could contribute to mTBI and may normally be excluded from a traditional video analysis of head impact events.

For the KTH FE head model results, the MPS values in Figure 11 shows the distribution between the two impact types. A statistical analysis revealed no significant difference in the mean values of the 95th percentile MPS. Typically, values above 0.2 MPS are associated with a milder level of mTBI and with a mean of 0.15 and a standard deviation of 0.21, these results indicated that even impacts with no direct head contact could contribute

to a player's accumulation of mTBI during game play. The detailed KTH simulations of the 50th and 99th percentile samples also showed similar results in Figure 16 and Figure 17. It is worth highlighting the different spatial distribution of the MPS results for both the standard KTH model in Figure 14 and Figure 15 and the detailed KTH model in Figure 18. The strains from impacts with no direct head contact appeared to be more present in the internal regions of the brain matter compared to the direct head impacts. While this can also be explained by the small dataset used, given that the impulse waves of an impact originating away from the head would need to travel up through the neck, this increased level of internal strains could be explained by this alternate path of momentum transfer within the players' body. An analysis of the top 10% of the events with highest peak linear acceleration show in all cases that the player received contact to their chest. In one case this was from a teammate handing the ball during a running pass, in the others this was from deflecting an oncoming tackle. It is possible that this large contact force results in a moment about the player's neck inducing a large acceleration in the head. This form of tackle whiplash should also be monitored carefully as other forms of whiplash injuries are present in other areas of human movement.

This data suggests that impacts with and without head involvement may be comparably capable of producing mTBI, however a key limitation is the size of the dataset used. This modest sample size was the result of the stringent requirement of clear classification of impact type. Improvements to this work could include further increasing the size of the dataset with improved video analysis to find more events of each type from practice and game sessions, as well as implementing a more detailed differentiation of the types of impacts with no head contact (i.e. does pushing or pulling result in worse kinematics compared to tackling a running player?). Another key issue with these results is the validity of the onscreen play and the associated impact data. Often the player will place their mouthguard in their sock or somewhere on their person and invalidate the true-seeming impact. This could be further improved with mouthguard design and more thorough video analysis, at the cost of increased manual labor. We also only included impacts where clear helmet-to-helmet contact visible in our dataset of direct head impacts, and it is possible that a more diverse group of direct head impacts including those where an athlete's head purely made contact with the ground or an opposing player's shoulder, torso, or limbs, could have altered the mean magnitude of this category of impacts. For example, helmet-to-ground and helmet-to-shoulder impacts have been found to be particularly prevalent in cases of diagnosed concussion in the National Football League ¹⁰ Further, many of our direct head impacts included a body-to-body component (e.g., pushing, grabbing, shoulder-to-shoulder contact) and it is possible that this contact contributed to the observed head kinematics. Therefore, it should not be assumed that head kinematics observed in the direct head impacts category were solely induced head helmet-to-helmet contact. Finally, we did not take note of player positions, session type (i.e., game or practice), or strategic play type. These factors, as well as other sport- or individual-specific factors, have been found to influence the magnitude of American football impacts ³³⁻³⁵ and our lack of controlling for these may have influenced the presented results.

Despite the modest dataset size and the binary distinction of impacts with and without direct head involvement, the results shown in this work prompt an important motivation moving forward when analyzing player data. While direct head impacts will remain the focus of m/TBI monitoring, with the increased adoption of instrumented sensors and improved video analysis, the authors hope that this work has shown that all impact events, including those without direct head contact, should not be discounted as impact events for players and should be solely judged on the kinematics measured, regardless of where the contact originated.

Conclusion

In this work datasets of impacts with and without direct head contact were collected and compared from collegiate American Football players. These datasets were gathered using a state-of-the-art impact detection algorithm embedded in an instrumented mouthguard to record head kinematics. Video analysis was used to differentiate between impact types. In total, 15 impacts of each type were used in comparison. Analysis of the kinematics showed that the impacts without direct head contact achieved similar levels of linear and angular accelerations during impact compared to those from direct head impacts. Finite element analyses were performed on the median and peak kinematic signals from each dataset to calculate maximum principal strain of the brain. Statistical analysis revealed that no significant difference was found between the two datasets based on a Bonferroni-adjusted p-value threshold of 0.017 p-value threshold of 0.05, with the exception of peak linear acceleration. Impacts without direct head contact showed higher mean values of peak linear acceleration values of 17.6 g compared to the direct-head impact mean value of 6.1g. These results indicated that impacts other than direct head impacts could still produce meaningful kinematic loads in the head and as such should be included in athlete health research.

References

1. Sahler CS, Greenwald BD. Traumatic Brain Injury in Sports: A Review. Ambrose AF, ed. *Rehabilitation Research and Practice*. 2012;2012:659652. doi:10.1155/2012/659652
2. Meaney DF, Smith DH. Biomechanics of Concussion. *Clinics in Sports Medicine*. 2011;30(1). doi:10.1016/j.csm.2010.08.009
3. Tator CH. Concussions and their consequences: Current diagnosis, management and prevention. *CMAJ*. 2013;185(11). doi:10.1503/cmaj.120039
4. McInnes K, Friesen CL, MacKenzie DE, Westwood DA, Boe SG. Mild Traumatic Brain Injury (mTBI) and chronic cognitive impairment: A scoping review. *PLoS ONE*. 2017;12(4). doi:10.1371/journal.pone.0174847

5. Gardner RC, Yaffe K. Epidemiology of mild traumatic brain injury and neurodegenerative disease. *Molecular and Cellular Neuroscience*. 2015;66(PB). doi:10.1016/j.mcn.2015.03.001
6. Beckwith JG, Greenwald RM, Chu JJ, et al. Head impact exposure sustained by football players on days of diagnosed concussion. *Medicine and Science in Sports and Exercise*. 2013;45(4). doi:10.1249/MSS.0b013e3182792ed7
7. O'Connor KL, Rowson S, Duma SM, Broglio SP. Head-impact-measurement devices: A systematic review. *Journal of Athletic Training*. 2017;52(3). doi:10.4085/1062-6050.52.2.05
8. Camarillo DB, Shull PB, Mattson J, Shultz R, Garza D. An instrumented mouthguard for measuring linear and angular head impact kinematics in american football. *Annals of Biomedical Engineering*. 2013;41(9). doi:10.1007/s10439-013-0801-y
9. Lucke-Wold B, Pierre K, Dawoud F, Gutierrez M. Changing the Culture: Improving Helmet Utilization to Prevent Traumatic Brain Injury. *Journal of emergency medicine forecast*. 2020;3(1).
10. Lessley DJ, Kent RW, Funk JR, et al. Video Analysis of Reported Concussion Events in the National Football League During the 2015-2016 and 2016-2017 Seasons. *American Journal of Sports Medicine*. 2018;46(14). doi:10.1177/0363546518804498
11. Lessley DJ, Kent RW, Cormier JM, et al. Position-Specific Circumstances of Concussions in the NFL: Toward the Development of Position-Specific Helmets. *Annals of Biomedical Engineering*. 2020;48(11). doi:10.1007/s10439-020-02657-z
12. Liu Y, Zhan X, Domel AG, et al. Theoretical and numerical analysis for angular acceleration being determinant of brain strain in mTBI. *arXiv preprint arXiv:201213507*. Published online 2020.
13. Smith TA, Halstead PD, McCalley E, Kebschull SA, Halstead S, Killeffer J. Angular head motion with and without head contact: implications for brain injury. *Sports Engineering*. 2015;18(3). doi:10.1007/s12283-015-0175-5
14. McCrory P, Meeuwisse W, Dvorak J, et al. Consensus statement on concussion in sport—the 5th international conference on concussion in sport held in Berlin, October 2016. *British Journal of Sports Medicine*. 2017;51(11):838. doi:10.1136/bjsports-2017-097699
15. Cassoude-salle H, Laborde B, Orhant E, Dehail P. Video analysis of concussion mechanisms and immediate management in French men's professional football (soccer) from 2015 to 2019. *Scandinavian Journal of Medicine and Science in Sports*. 2021;31(2). doi:10.1111/sms.13852
16. Caswell S v., Kelshaw PM, Lincoln AE, et al. The Effects of Headgear in High School Girls' Lacrosse. *Orthopaedic Journal of Sports Medicine*. 2020;8(12). doi:10.1177/2325967120969685
17. Cecchi NJ, Monroe DC, Fote GM, Small SL, Hicks JW. Head impact exposure and concussion in women's collegiate club lacrosse. *Research in Sports Medicine*. Published online 2021. doi:10.1080/15438627.2021.1929226

18. Jadischke R, Viano DC, McCarthy J, King AI. Concussion with primary impact to the chest and the potential role of neck tension. *BMJ Open Sport and Exercise Medicine*. 2018;4(1). doi:10.1136/bmjsem-2018-000362
19. Liu Y, Domel AG, Cecchi NJ, et al. Time Window of Head Impact Kinematics Measurement for Calculation of Brain Strain and Strain Rate in American Football. *Annals of Biomedical Engineering*. Published online 2021. doi:10.1007/s10439-021-02821-z
20. Domel AG, Raymond SJ, Giordano C, et al. A new open-access platform for measuring and sharing mTBI data. *Scientific Reports*. 2021;11(1):7501. doi:10.1038/s41598-021-87085-2
21. Raymond SJ, Camarillo DB. Applying physics-based loss functions to neural networks for improved generalizability in mechanics problems. Published online April 30, 2021. Accessed August 2, 2021. <http://arxiv.org/abs/2105.00075>
22. Raymond SJ, Collins DJ, O'Rourke R, Tayebi M, Ai Y, Williams J. A deep learning approach for designed diffraction-based acoustic patterning in microchannels. *Scientific reports*. 2020;10(1):1-12.
23. Kuo C, Wu L, Loza J, Senif D, Anderson SC, Camarillo DB. Comparison of video-based and sensor-based head impact exposure. *PLoS ONE*. 2018;13(6). doi:10.1371/journal.pone.0199238
24. Kleiven S. Predictors for traumatic brain injuries evaluated through accident reconstructions. *Stapp car crash journal*. 2007;51.
25. Hardy WN, Mason MJ, Foster CD, et al. A study of the response of the human cadaver head to impact. *Stapp car crash journal*. 2007;51.
26. Nahum AM, Smith R, Ward CC. Intracranial pressure dynamics during head impact. In: *SAE Technical Papers*. ; 1977. doi:10.4271/770922
27. Zhou Z, Li X, Kleiven S, Hardy WN. Brain Strain from Motion of Sparse Markers. *Stapp car crash journal*. 2019;63. doi:10.4271/2019-22-0001
28. Zhan X, Liu Y, Raymond SJ, et al. Rapid Estimation of Entire Brain Strain Using Deep Learning Models. *IEEE Transactions on Biomedical Engineering*. Published online 2021:1. doi:10.1109/TBME.2021.3073380
29. Zhan X, Li Y, Liu Y, et al. The relationship between brain injury criteria and brain strain across different types of head impacts can be different. *Journal of The Royal Society Interface*. 2021;18(179):20210260. doi:10.1098/rsif.2021.0260
30. Li X, Zhou Z, Kleiven S. An anatomically detailed and personalizable head injury model: Significance of brain and white matter tract morphological variability on strain. *Biomechanics and Modeling in Mechanobiology*. 2021;20(2). doi:10.1007/s10237-020-01391-8
31. Zhou Z, Domel AG, Li X, et al. White matter tract-oriented deformation is dependent on real-time axonal fiber orientation. *Journal of Neurotrauma*. 2021;38(12). doi:10.1089/neu.2020.7412
32. Zhou Z, Li X, Liu Y, et al. Towards a comprehensive delineation of white matter tract-related deformation. *bioRxiv*. Published online January 1, 2021:2021.04.13.439136. doi:10.1101/2021.04.13.439136

33. Crisco JJ, Wilcox BJ, Beckwith JG, et al. Head impact exposure in collegiate football players. *Journal of Biomechanics*. 2011;44(15). doi:10.1016/j.jbiomech.2011.08.003
34. Broglio SP, Sosnoff JJ, Shin SH, He X, Alcaraz C, Zimmerman J. Head impacts during high school football: A biomechanical assessment. *Journal of Athletic Training*. 2009;44(4). doi:10.4085/1062-6050-44.4.342
35. Reynolds BB, Patrie J, Henry EJ, et al. Practice type effects on head impact in collegiate football. *Journal of Neurosurgery*. 2016;124(2). doi:10.3171/2015.5.JNS15573